Supporting Information for

Spontaneous Patterning during Frontal Polymerization

Evan M. Lloyd, Elizabeth C. Feinberg, Yuan Gao, Suzanne R. Peterson, Bhaskar Soman, Julie Hemmer, Leon M. Dean, Qiong Wu, Philippe H. Geubelle*, Nancy R. Sottos*, Jeffrey S. Moore*

Correspondence to: jsmoore@illinois.edu, n-sottos@illinois.edu, geubelle@illinois.edu

Table of Contents

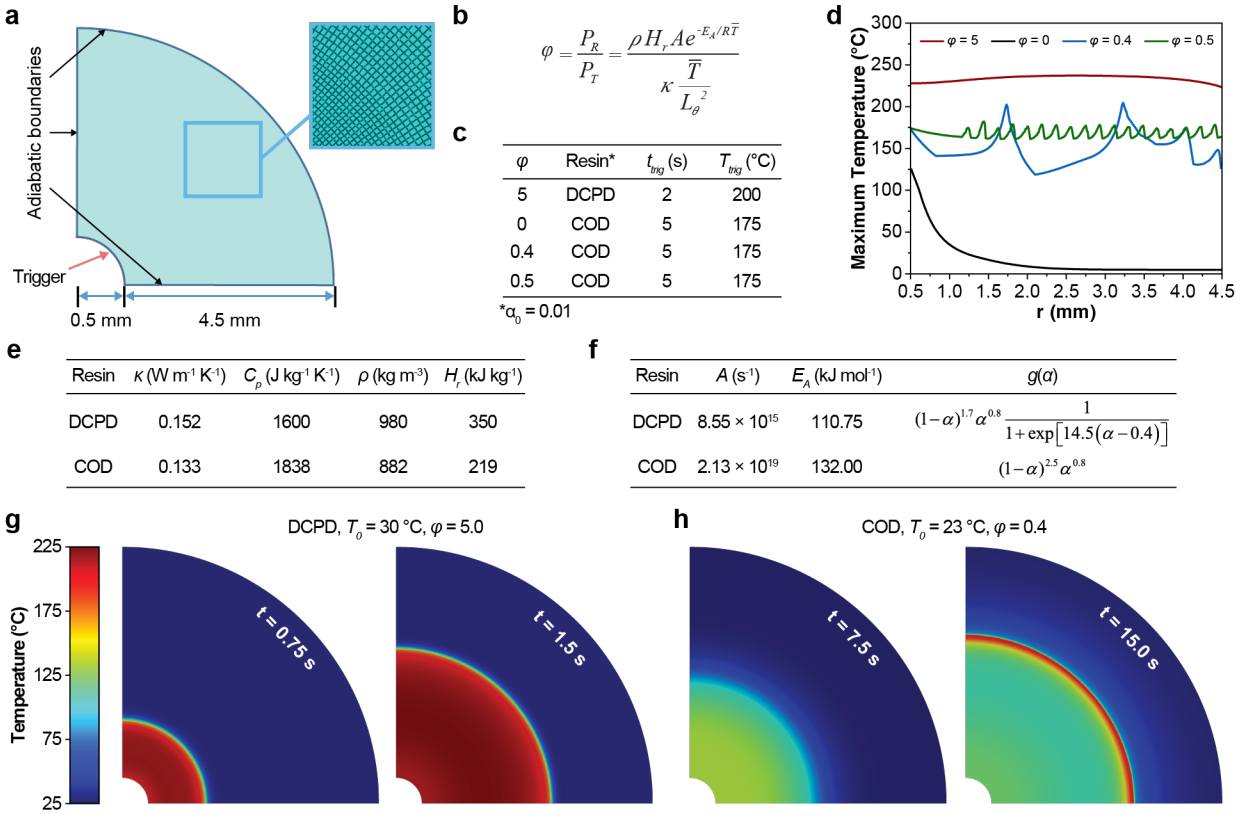

φ	Resin*	t_{trig} (s)	T_{trig} (°C)
5	DCPD	2	200
0	COD	5	175
0.4	COD	5	175
0.5	COD	5	175

*α_0 = 0.01

Resin	κ (W m^{-1} K^{-1})	C_p (J kg^{-1} K^{-1})	ρ (kg m^{-3})	H_r (kJ kg^{-1})
DCPD	0.152	1600	980	350
COD	0.133	1838	882	219

Resin	A (s^{-1})	E_A (kJ mol^{-1})	$g(\alpha)$
DCPD	8.55×10^{15}	110.75	$(1-\alpha)^{1.7}\alpha^{0.8}\frac{1}{1+\exp[14.5(\alpha-0.4)]}$
COD	2.13×10^{19}	132.00	$(1-\alpha)^{2.5}\alpha^{0.8}$

Figure S1. Numerical simulation of frontal polymerization. (a) Schematic representation of the axisymmetric model of frontal polymerization in a quarter fan-shaped domain. Inset represents a schematic of the mesh utilized to discretize the domain. (b) Ratio of power density (φ) generated by reaction (P_R) and spread by thermal transport (P_T) during frontal polymerization. ρ, H_r, A, E_A, R, $\bar{T}$, κ, and L_θ represent the density of the resin, heat of reaction, activation energy, universal gas constant, average of the maximum and initial temperature, and the width of the thermal front, respectively. (c) Polymerization trigger conditions (expressed in terms of the temperature T_{trig} applied over a duration t_{trig}) used for various values of φ. (d) Radial profiles of maximum temperature computed for various values of φ. (e) Material properties of dicyclopentadiene and cyclooctadiene used in the computational models. (f) Cure kinetic parameters obtained by fitting dynamic DSC traces. (g,h) Evolution of the polymerization front in DCPD and COD.

Figure S1b provides the formal definition of the spatiotemporal balance of power density, φ, generated by the reaction and spread by thermal transport, analogous to the Damköhler number utilized throughout chemical engineering literature[1]. **Figure S1d** shows the radial variation of the maximum temperature, T_{max}, predicted by numerical analysis, which is a quantitative description of **Figure 1c**. When $\varphi \approx 0$, frontal polymerization is unable to initiate, and T_{max} decreases from T_{trig} to T_0 as r increases. When $\varphi = 0.4$, several peaks of T_{max} at different r are obtained, reflecting

the unstable propagation of the front. The magnitude and wavelength of the peaks in T_{max} decreases when $\varphi = 0.5$, indicating an increase in stability. At $\varphi = 5$, no peaks in T_{max} are observed, indicating stable front propagation. **Figure S1g,h** demonstrate snapshots of numerical simulation of stable and unstable front propagation, respectively.

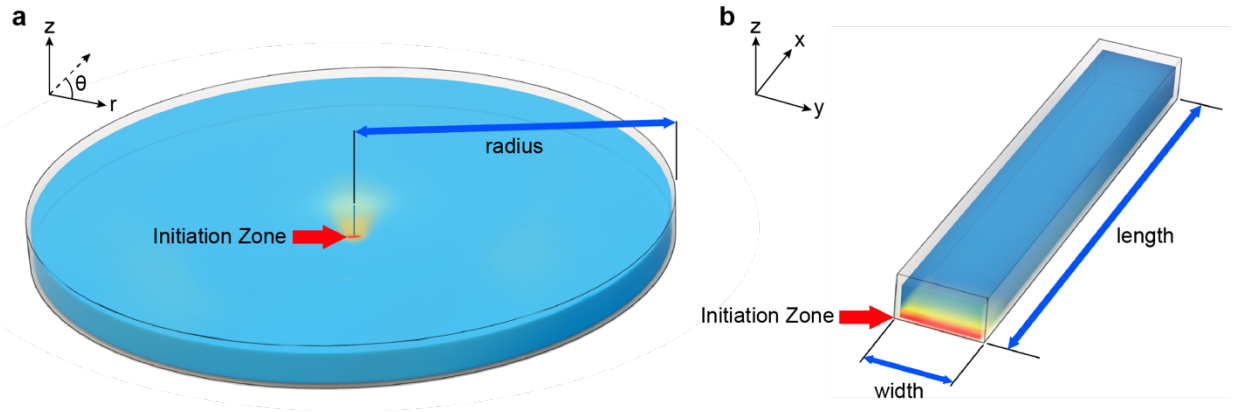

Figure S2. Experimental mold geometry. (a,b) Schematic representation of cylindrical (a) and channel (b) molds. Initiation was achieved by powering a resistive wire in contact with the molds at the indicated locations.

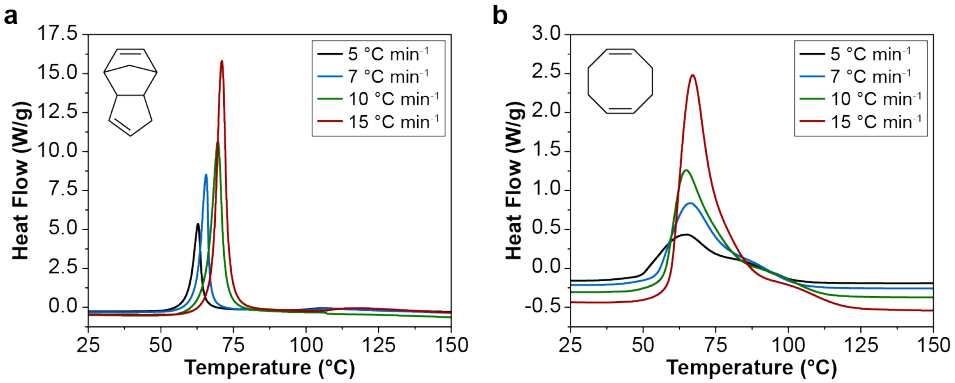

Figure S3. Characterization of DCPD and COD curing. (a,b) Dynamic DSC traces for DCPD (a) and COD (b) obtained at various ramp rates. Onset of initiation ranges between 55 and 65 °C for DCPD and 50 and 60 °C for COD, dependent upon ramp rate. Data in b was adapted from Dean et al.[2]

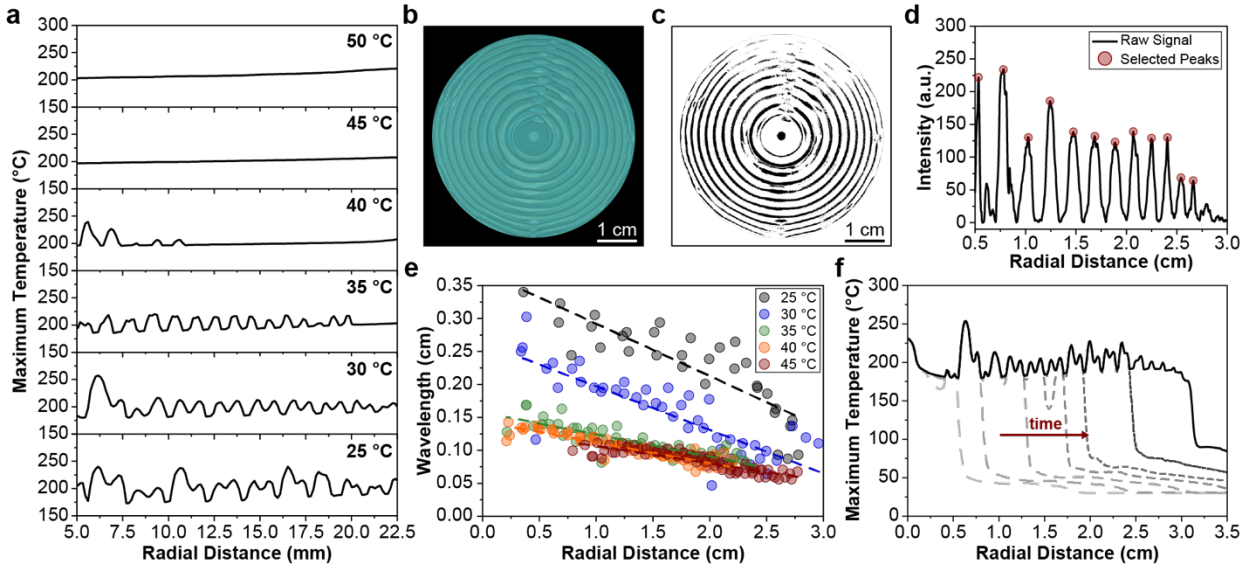

Figure S4. Characterization of DCPD circumferential propagation. (a) Representative maximum temperature profiles obtained for various initial resin temperatures (T_0). Data represent measurements along a single radial line. (b) Representative fluorescent image of a pDCPD sample (T_0 = 30 °C) used for wavelength analysis. (c) Result of binary conversion, pixel erosion, and pixel dilation of the image depicted in b. (d) Radial intensity profile of the binary image in c with the peaks selected to calculate the feature wavelength depicted in red. (e) Feature wavelength as a function of radial distance at various initial temperatures. Both initial wavelength and the wavelength decay constant (defined as the slope of the linear fits) decrease with increasing initial temperature. (f) Representative maximum temperature profiles at various time points after initiation. The temperature of the monomer ahead of the polymerization front steadily increases with increasing time, which contributes to the decay in feature wavelength.

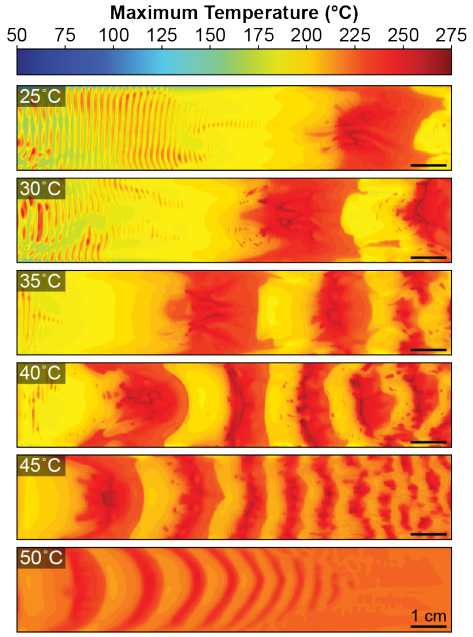

Figure S5. Tuning of thermal profiles during free-surface FROMP of DCPD. Maximum temperature profiles obtained with various initial resin temperatures. Feature size and spacing decrease with increasing initial resin temperature.

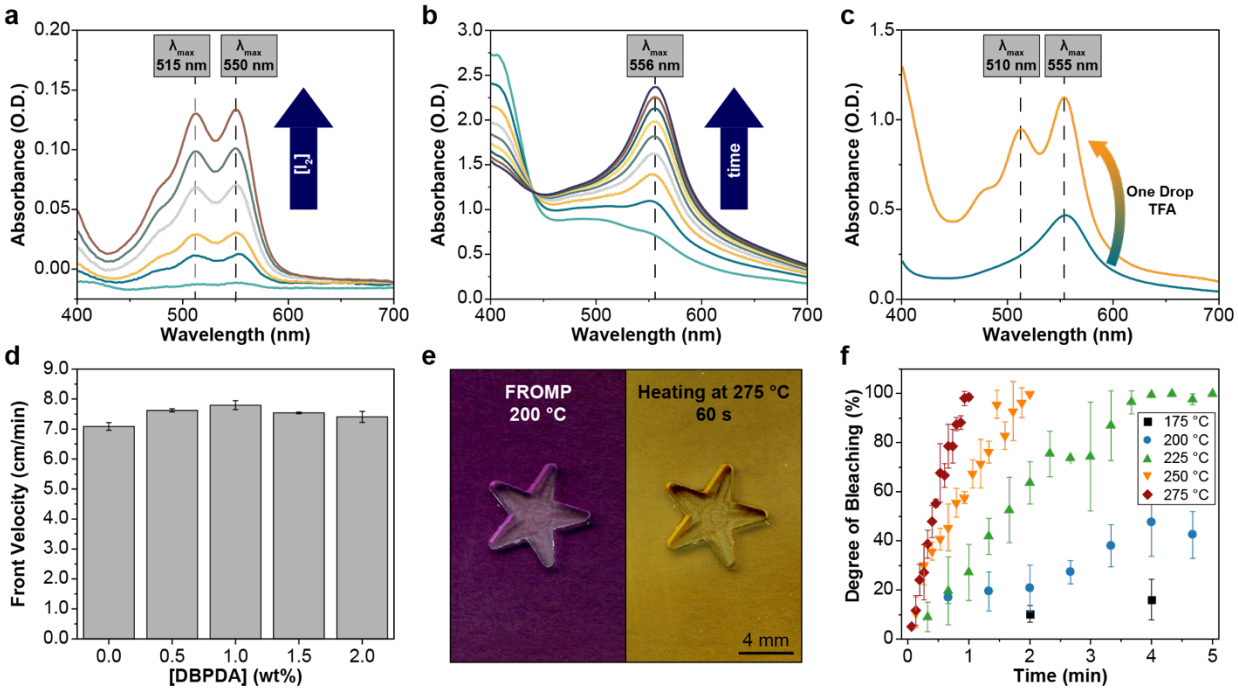

Figure S6. Characterization of DBPDA thermochromes. (a) UV-Vis absorption spectra of DBPDA treated with increasing amounts of iodine in dichloromethane, showing the characteristic absorption spectrum of the *p*-phenylenediamine radical cation[3,4]. (b) Evolution of the absorption spectra (obtained at 2 min intervals) of DBPDA treated with 0.075 molar equivalents of Grubbs catalyst 2nd generation (GC2) in dichloromethane. (c) Absorption spectrum obtained after treatment of a solution of DBPDA and GC2 in dichloromethane with a single drop of trifluoroacetic acid (TFA), demonstrating clean formation of the DBPDA radical cation. It is believed that GC2 facilitates the formation of a DBPDA radical cation dimer, which is disrupted by the addition of acid. (d) Front velocities obtained with various concentrations of DBPDA. The presence of DBPDA has minimal impact on frontal propagation. (e) Optical images of a sample loaded with 2 wt% DBPDA after frontal propagation in a mold with a star shaped projection at 200 °C (temperature confirmed with a thermocouple submerged in resin) (left) and after heating on a metal substrate maintained at 275 °C for 60 s. The presence of a deep purple color is indicative of radical cation formation during mild temperature front propagation, while the return to the native yellow color of pDCPD is suggestive of radical cation fragmentation to colorless species. (f) Ex situ bleaching of pDCPD samples containing 2 wt% DBPDA after heating on a hot stage at the indicated temperature. Degree of bleaching was determined by analyzing the yellow channel of optical images of the heated samples. Rapid bleaching is observed at temperatures in excess of 250 °C.

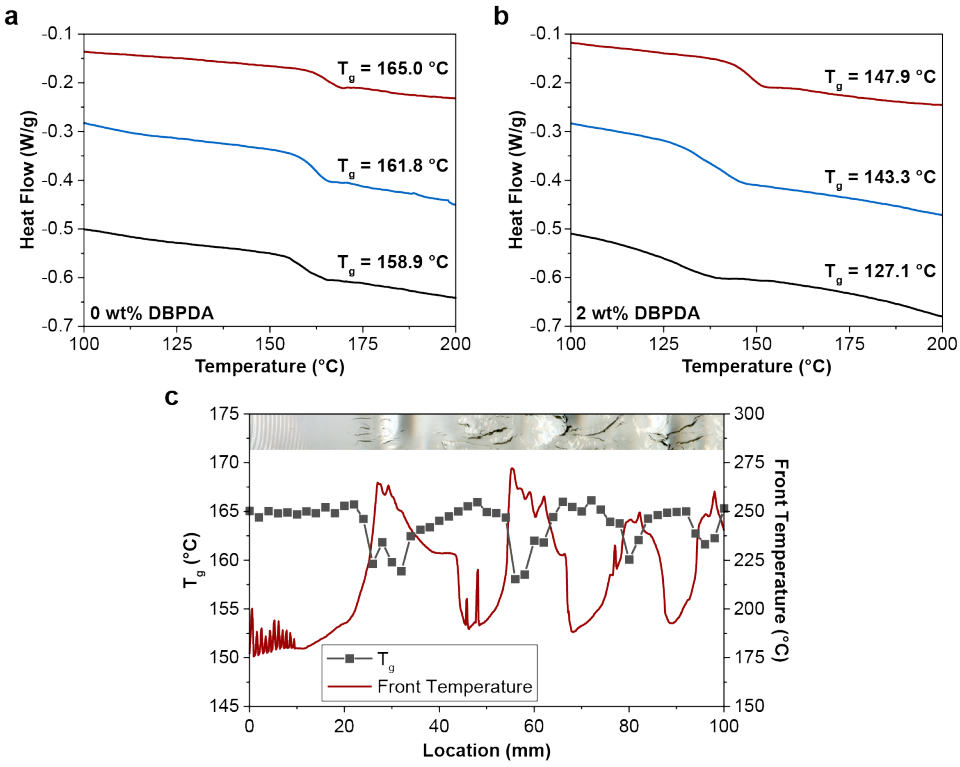

Figure S7. Thermomechanical properties of pDCPD obtained after free-surface FROMP. (a,b) Representative DSC traces of pDCPD containing containing 0 wt% (a) and 2 wt% (b) DBPDA. Tested samples experienced varied front temperature. High T_g traces experienced front temperatures near 200 °C; low T_g traces experienced front temperatures near 270 °C. (c) Glass transition temperature and maximum front temperature of a sample containing 0 wt% DBPDA. Inset represents an optical image of the tested region.

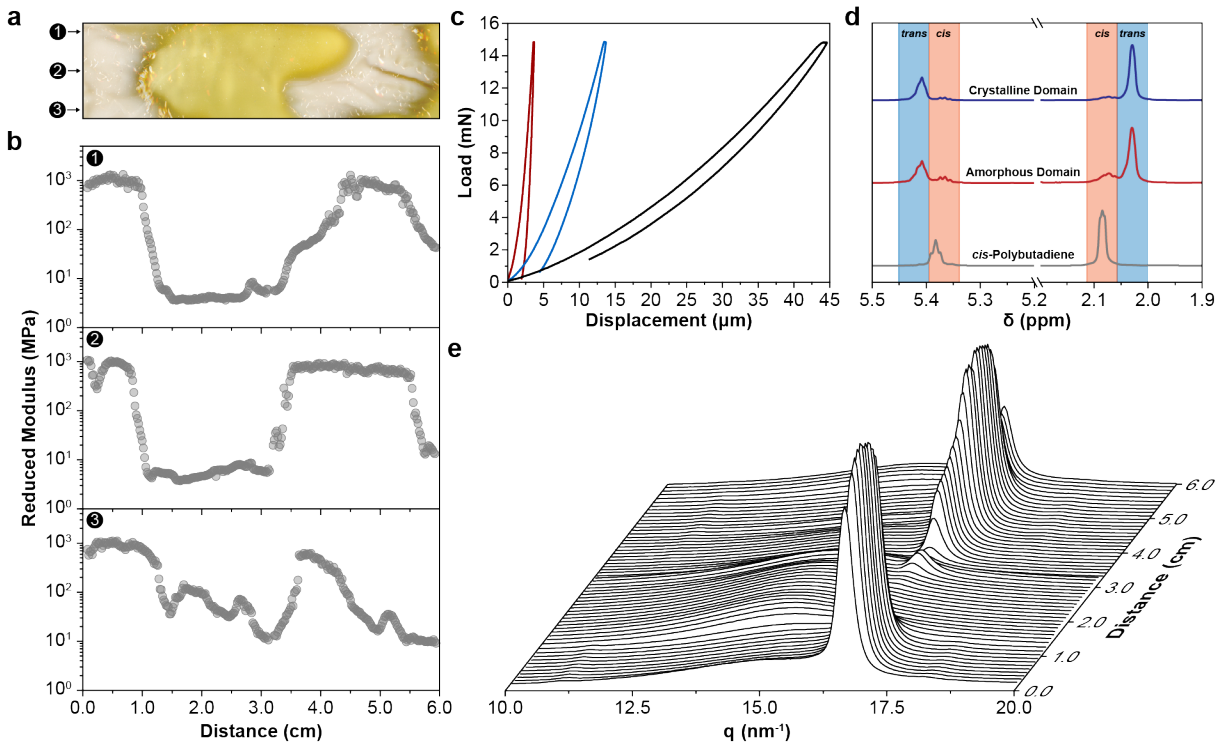

Figure S8. Characterization of pCOD. (a) Optical image of pCOD obtained after free-surface FROMP with an initial resin temperature of 30 °C. (b) Reduced modulus as a function of distance from the initiation zone obtained via nanoindentation. Data were obtained with linear scans along the length of the sample starting at the indicated locations and correlated to the maximum front temperature to provide the data depicted in **Figure 4e**. (c) Representative load-displacement curves obtained during indentation of the specimen shown in a. Reduced modulus was extracted by fitting the unloading curve with Oliver-Pharr method[5]. (d) ^{1}H NMR spectra (500 MHz, chloroform-*d*) of a *cis*-polybutadiene standard and the soluble fractions from the crystalline and amorphous domains shown in a. Chloroform-*d* was treated with 1 vol% ethyl vinyl ether prior to the addition of samples to quench residual GC2 and prevent isomerization upon dissolution. Peaks corresponding to ethyl vinyl ether are omitted for clarity. The crystalline domain was fully soluble and contained 88% *trans* alkenes while the amorphous domain was only partially soluble, with the soluble fraction containing 76% *trans* alkenes. (e) WAXS spectra obtained along the length of the sample in a starting at location 1. Crystalline domains are marked by a sharp peak at a scattering vector of 16.7 nm^{-1}, while amorphous domains only contain an amorphous halo. The transition regions experience a sharp decrease in the peak at 16.7 nm^{-1}.

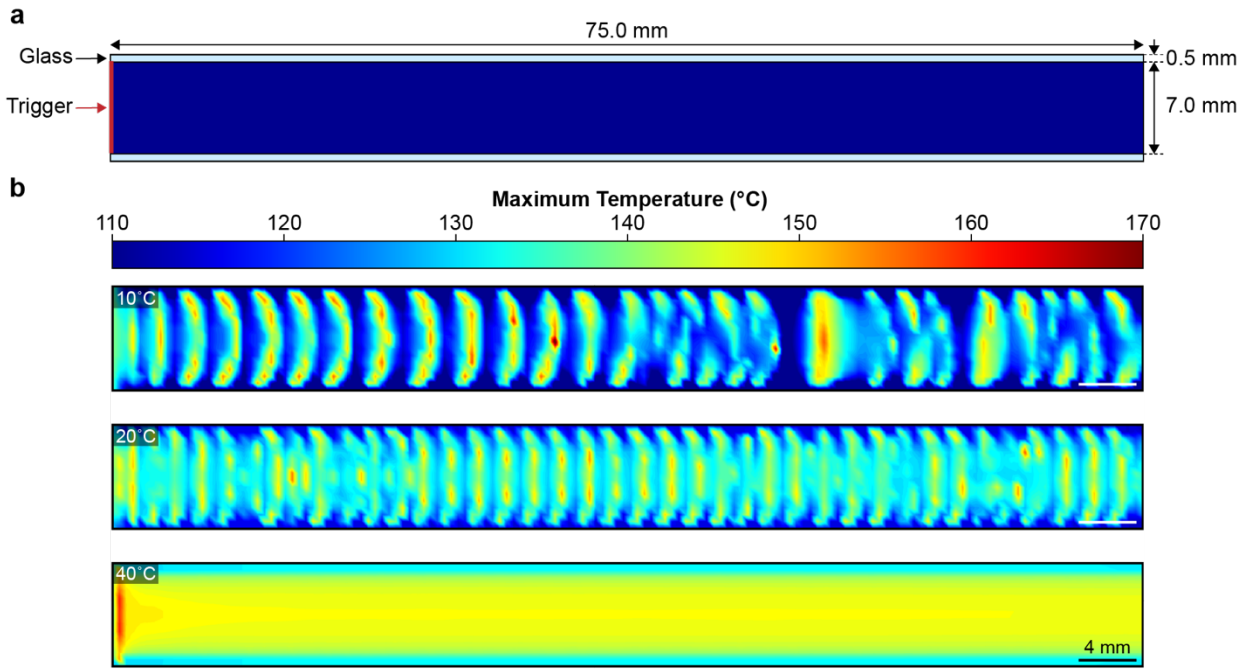

Figure S9. Numerical simulation of COD frontal polymerization in a channel geometry. (a) Schematic representation of the frontal polymerization in a channel domain with glass boundaries. (b) Maximum temperature profiles obtained with various initial resin temperatures. The solution of the reaction-diffusion equations captures the FP-induced thermal instabilities and the resulting pattern complexity that decreases with increasing initial resin temperature.

Figure S9b shows the maximum temperature profiles computed for COD when the front propagates in a long glass channel. The symmetry of frontal propagation and the resulting pattern size, spacing, and shape are readily tuned by varying the initial temperature of the resin, T_0. At high initial temperatures, e.g. T_0 = 40 °C, fronts propagate in a steady fashion, and the resulting temperature profile is homogeneous. At reduced initial temperatures, e.g. $T_0 \leq 20$ °C, propagating fronts display symmetry breaking events, leading to striped patterns that increase in complexity with distance from the initiation point.

Video Captions

Video S1. Circumferential propagation is observed during FROMP of DCPD in an open circular mold and generates patterned thermal profiles. Monomer is spontaneously heated ahead of the polymerization front by thermal transport, and subsequent circumferential propagation consumes the heated monomer. The resin is maintained at 30 °C prior to initiation with a resistive wire. The video is presented at 1× speed, and maximum front temperature is shown for clarity. The scale bar is 1 cm.

Video S2. During free-surface FROMP of DCPD in rectangular channels, thermal transport spontaneously heats a large region of monomer, which is subsequently consumed in a rapid, high temperature polymerization reaction. Spontaneous heating and rapid consumption of monomer repeat cyclically to generate a striped thermal profile. The monomer is maintained at 40 °C prior to initiation with a resistive wire. The video is presented at 2× speed, and maximum front temperature is shown for clarity. The scale bar is 1 cm.

Video S3. During free-surface FROMP of COD in rectangular channels, thermal transport spontaneously heats a large region of monomer, which is subsequently consumed in a rapid, high temperature polymerization reaction. Spontaneous heating and rapid consumption of monomer repeat cyclically to generate a patterned thermal profile. The monomer is maintained at 30 °C prior to initiation with a resistive wire. The video is presented at 2.5× speed, and maximum front temperature is shown for clarity. The scale bar is 1 cm.

References

1. Fogler, H. S. *Elements of Chemical Reaction Engineering* Forth Edition. Prentice Hall: Upper Saddle River, NJ, **2006**.
2. Dean, L. M.; Wu, Q.; Alshangiti, O.; Moore, J. S.; Sottos, N. R. Rapid Synthesis of Elastomers and Thermosets with Tunable Thermomechanical Properties. *ACS Macro Lett.* **2020**, 9, 819-824.
3. Chung, Y.-C.; Su, Y. O. Effects of Phenyl- and Methyl-Substituents on *p*-Phenylenediamine, an Electrochemical and Spectral Study. *J. Chin. Chem. Soc.* **2009**, 56, 493-503.
4. Michaelis, L.; Schubert, M. P.; Granick, S. The Free Radicals of the Type of Wurster's Salts. *J. Am. Chem. Soc.* **1939**, 61, 1981–1992.
5. Oliver, W. C.; Pharr, G. M. An Improved Technique for Determining the Hardness and Elastic Modulus Using Load and Displacement Sensing Indentation Experiments. *J. Mater. Res.* **1992**, 7, 1564-158.